

THE CMS EXPERIMENT AT THE LHC

DANIEL DENEGRI^a, NIKOLA GODINOVIĆ^b, IVICA PULJAK^b, ŽELJKO
ANTUNOVIĆ^c and MILE DŽELALIJA^c,
for the CMS Collaboration

^a*DAPNIA/SPP, CE Saclay, Gif-sur-Yvette, France*

^b*University of Split, Faculty of Electrical Engineering, Mechanical Engineering and Naval
Architecture, Split, Croatia*

^c*University of Split, Faculty of Natural Sciences, Mathematics and Education, Split,
Croatia*

Dedicated to the memory of Professor Dubravko Tadić

Received 27 June 2005; Accepted 12 November 2005
Online 6 February 2006

We discuss the current status of the Large Hadron Collider (LHC) machine, the progress on the construction of the CMS detector and some expectations for physics studies and searches at the LHC.

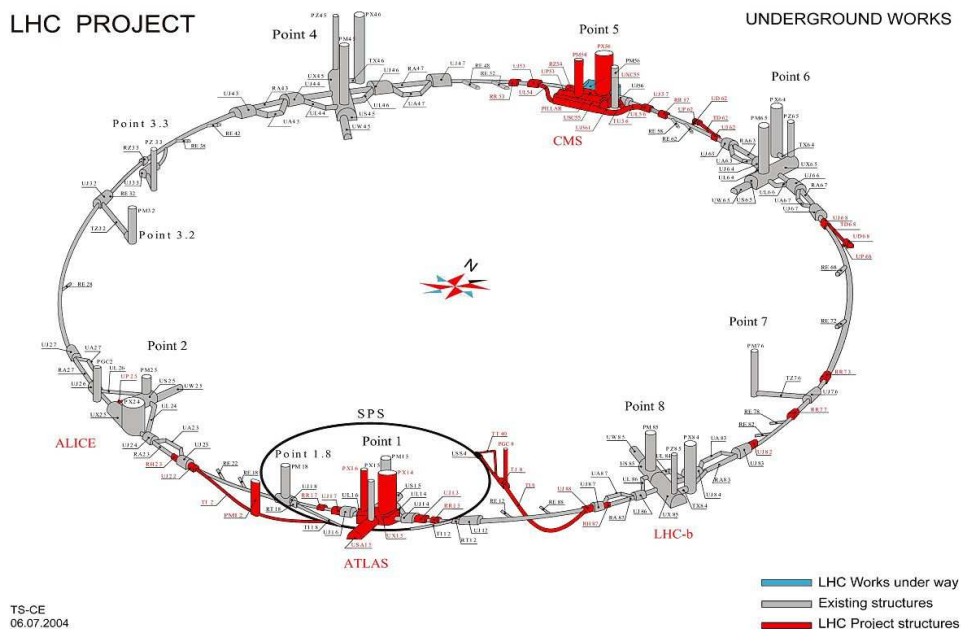
PACS numbers: 29.20.Lq, 29.40.Gx, 12.60.Fr, 14.80.Bn, 14.80.Ly; UDC 539.126, 539.127

Keywords: LHC, CMS, stage of construction, electroweak symmetry breaking, generation of particle masses, Higgs mechanism, supersymmetric particles

1. Introduction

The Large Hadron Collider (LHC) and the experiments, now at an advanced stage of construction at CERN, will be the key instruments of particle physics research in the coming years. The main motivation to build the LHC is the study of the mechanism responsible for electroweak symmetry breaking and generating particle masses, in the Standard Model (SM) the Higgs mechanism [1] with a single Higgs boson H . In Supersymmetry (SUSY), the particle spectrum is essentially doubled through the introduction of supersymmetric partners to known SM particles, and the Higgs sector is extended to at least five Higgs bosons in the Minimal Supersymmetric Standard Model (MSSM) [2]. The search for the possible supersymmetric partners of SM particles will be among the highest priorities at the LHC. New ideas, which could provide an alternative solution to the energy (mass) scale hierarchy problem, invoking existence of extra (possibly large) dimensions, have emerged recently [3]. Investigations of possible experimental manifestations of these extra dimensions will also be most actively pursued at the LHC.

Two general-purpose detectors, ATLAS [4] and CMS [5], will be installed at the LHC (Fig. 1). The construction, installation and commissioning of parts of these detectors is now proceeding at full speed. The primary goals of these two experiments are the Higgs boson and SUSY searches and, naturally, detailed studies of QCD and the electroweak theory. Although the physics goals of these two detectors are very much the same, the detector designs and experimental techniques are different and complementary, in particular in the B -field configuration and calorimeter techniques. These detectors should be ready to take initial data (LHC test runs) by mid-2007. Two somewhat smaller-scale detectors will also be operating at LHC, the ALICE [6] detector devoted to studies of the expected quark-gluon plasma QCD phase in heavy ion collisions, and the LHC-B [7] detector specialized for B-physics and CP/B violation studies (Fig. 1). CMS has also a significant and original heavy-ion physics programme [8]. The construction of both LHCb and ALICE is also progressing, aiming at taking data in 2007/08.



TS-CE
06.07.2004

Fig. 1. LHC layout, with the four major experimental systems. The existing LEP tunnel and the additional underground civil engineering works required for the LHC and experiments is shown.

2. Status of LHC construction

In the 27 km long tunnel, where once the LEP was located, the installation of the LHC machine components, cryogenic lines, magnets etc. is now proceeding fast. The excavation of the large underground experimental halls for the CMS and ATLAS detectors and of the adjoining service caverns for electronics and computers

is finished. The ATLAS caverns were ready by mid-2003 and the ATLAS detector is at present being mounted in its underground experimental hall. As the CMS detector can be test-assembled in the surface experimental hall, this allowed for the underground caverns of CMS to be delivered later. The CMS experimental halls were delivered in February 2005, and the installation of infrastructure is going on. The CMS detector, now under assembly in its surface experimental hall, will be lowered through a large access shaft (Figs. 1 and 2) and reassembled in the underground experimental hall (Fig. 3) in mid-2006.



Fig. 2 (left). LHC point 5, with the 24 m diameter shaft to the CMS underground experimental hall and the cover.

Fig. 3. The underground CMS experimental hall, March 2005, the lower end of the access shaft is visible.

2.1. Status of machine construction

About 65% of the 27 km circumference of the LHC tunnel is to be covered twice with $B = 8.3$ T magnetic field with 1232 2-in-1 super-conducting dipoles of 14.3 m length, cooled at 1.9 K. There are also about 500 2-in-1 quadrupoles with a gradient of 250 T/m, ~ 4000 corrector sextupoles and octupoles, altogether 1200 tons of super-conducting cable and 40.000 tons of material at superfluid He temperature! The bending dipoles are the key elements of the LHC project. Dipole development and production took over 10 years. In 2001, five 15 m long 6-block coil dipoles have been tested and satisfactorily operated above 8.3 T, as well as three second-generation final design prototype dipoles. Subsequently, thirty final-design industrial pre-production dipoles have been ordered in 2001 from each of the three manufacturers: Noell, Alstom/Jeumont and Ansaldo. Tests gave excellent results, with the ultimate field of 9 T achieved after few training quenches. This pre-series production was completed in 2003. We are now in the final series-production phase, with 386 dipoles to be produced by each manufacturer. By the summer of 2005, about 700 cold masses will have been manufactured (Fig. 4) and about 500 complete dipoles assembled and tested at CERN (Figs. 5 and 6). Figure 7 shows LHC dipoles on test benches and the second LHC string test (now dismantled).

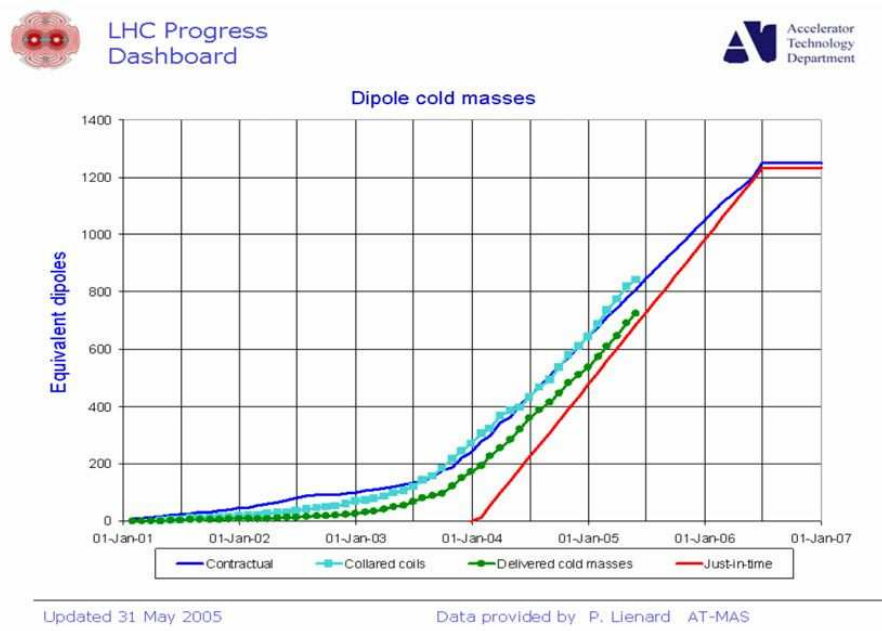


Fig. 4. Progress on the construction of main dipoles (cold masses) by mid-2005.



Fig. 5. Cryostating main dipoles at CERN.

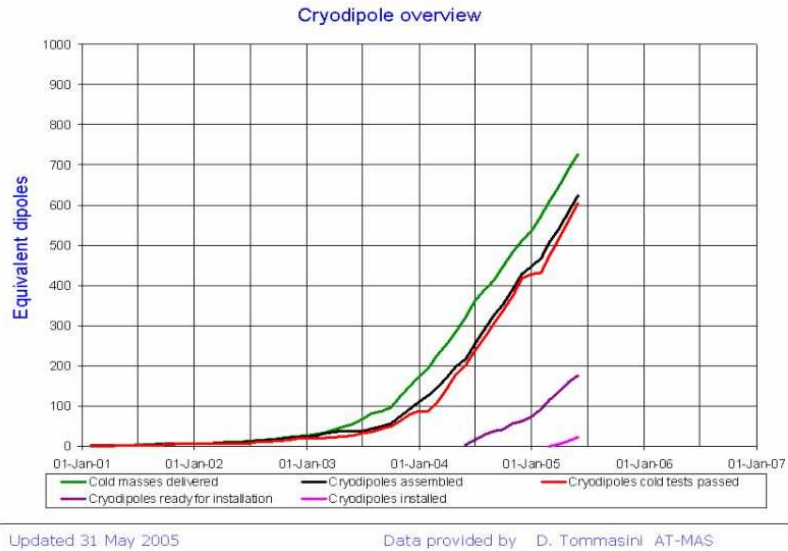


Fig. 6. Progress on the construction of complete main dipoles, up to mid-2004.



Fig. 7. LHC dipoles on test benches (center/left) and the LHC string test (right).

The first bending dipoles were lowered and installed in the tunnel in April 2005, once the problems with the modifications of the cryogenic cooling lines, which must be installed before magnets can be put in place in the tunnel, have been overcome. The present expectations are for the installation of the LHC magnets to go on till

the end of 2006, with machine cooled and commissioning in 2007. A first pilot run is expected in the second half of 2007.

3. CMS detector construction

3.1. Status of solenoid construction, yoke and coil

A longitudinal cut through the CMS detector is shown in Fig. 8. Central to the design of CMS is the 13.5 m long, 6.2 m inner diameter solenoid generating a uniform magnetic field of 4 T [9]. The magnetic flux is returned through iron discs in the endcaps and a 1.8 m thick saturated iron barrel yoke instrumented with muon chambers. The CMS magnetic return barrel yoke is the main structural element supporting the whole system. It is subdivided into 5 “wheels”, each of these iron wheels weighs about 1200 tons. The central wheel also supports the cryostat of the solenoid to which are attached the barrel hadronic and electromagnetic calorimeters. The barrel yoke structure has been completed and assembled in the surface hall of CMS in 2002.

The assembly of the 2×3 iron discs of the end-cap yoke has been completed



Fig. 8. Longitudinal cut through one quadrant of CMS; the barrel and endcap muon stations are denoted by MB and ME, the tower structure of the hadron calorimeter (HB, HE) and the arrangement of the electromagnetic calorimeter crystals (EB, EE) is indicated.

in 2003. The inner and outer coil vacuum tank cylindrical walls have been test mounted. Figure 9 shows the inner cryostat cylinder positioned for insertion into the central barrel wheel in a test performed in 2002. At present, summer 2005, the barrel muon stations are inserted in the gaps within the barrel yoke wheels, the endcap hadron calorimeters have also been mounted and the mounting of endcap

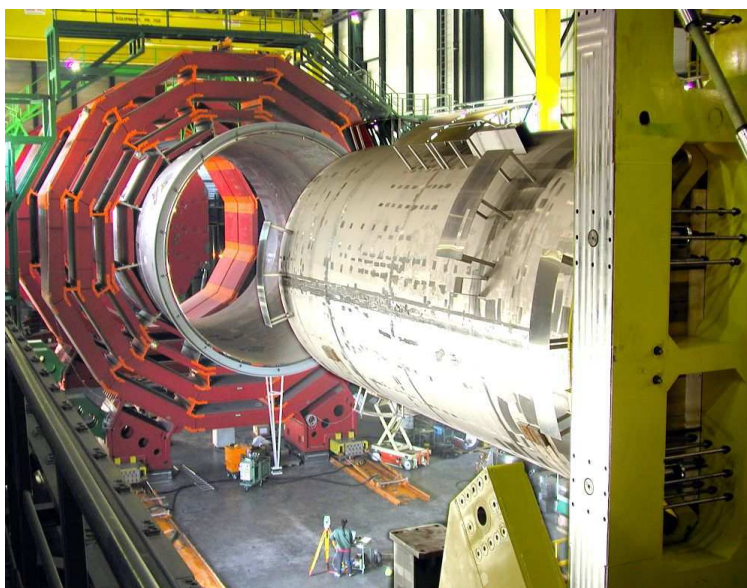


Fig. 9. The barrel return yoke, with the central “wheel” carrying the outer solenoid vacuum tank wall and insertion test of the inner cryostat wall.

muon stations on endcap yoke discs is going on. The operations of lowering the ~1200-ton “wheels” fully equipped with muon chambers 100 meters underground in the CMS experimental hall are scheduled for the first half of 2006.



Fig. 10. Five coil modules connected together in CMS surface experimental hall, spring 2005.

The construction of the CMS solenoid [9], with its four-layers winding to achieve the desired 4 Tesla field, is nearing completion. The coil was designed by CEA-Saclay and coil winding, now completed, was performed at Ansaldo (Genova), under the responsibility of the INFN-Italy. The conductor itself consists of three parts, an inner superconducting Rutherford cable surrounded by a pure aluminum layer for thermal and electric stabilization and an external aluminum-alloy layer for mechanical strength [9]. The transverse dimensions of the conductor are $22 \text{ mm} \times 64 \text{ mm}$. The total length of conductor is 53 km. Longitudinally, the solenoid is subdivided into five modules. The five coil modules have been completed and delivered to CERN, the last coil module in January 2005. Figure 10 shows the five coil modules being interconnected in the CMS surface experimental hall, and Fig. 11 the 20 kAmp bus-bars feeding the coil (Končar/Croatia) being installed in the underground area. Cool-down and tests of the magnet in the surface experimental hall of CMS are planned for the end of 2005 with field mapping and a cosmic ray test in a partially completed CMS detector in the first months of 2006.



Fig. 11. Passage of the 20 kA bus bars feeding the solenoid through the pillar wall.

3.2. Muon detection system

A robust muon-detection system is central to the CMS concept [5,10]. Muons provide the best signature for a number of physics signals, $H \rightarrow 4\mu^\pm$, $H_{\text{SUSY}} \rightarrow 2\mu^\pm, 4\mu^\pm$, sparticle signals, B-physics channels, $\psi, Y \rightarrow \mu^+\mu^-$ in pp, heavy ion collisions etc.

The CMS muon system has three purposes, to identify muons, to trigger and to measure their momenta. The precision momentum measurement comes from the inner tracking and the interconnection between inner and outer measurements. A barrel muon station consists of drift planes for precision measurements and one or

two resistive plane chambers (RPC's) on the outside for triggering [10], Figs. 8 and 12. There are 12 drift-tube layers per barrel muon station (Fig. 12), two quadruplets measuring in the bending plane ($r\phi$) and one the longitudinal (z) coordinate. A

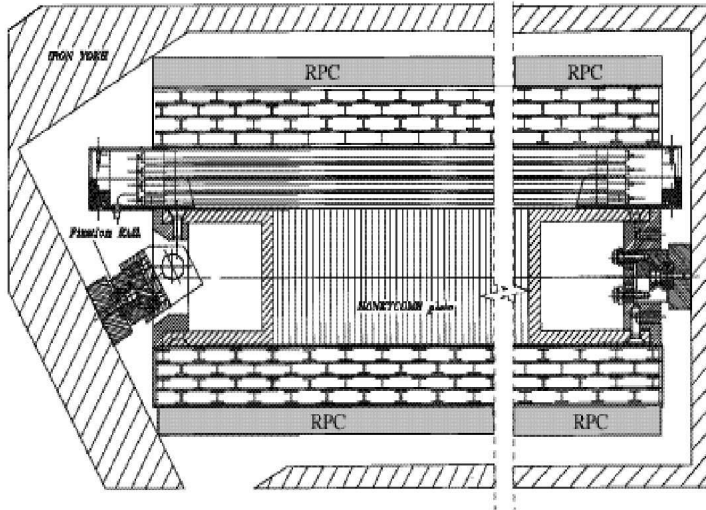


Fig. 12. Cross section of a barrel muon chamber in the $r\phi$ (bending) plane. The two drift tube superlayers with wires parallel to the beam line are seen face on, the z -layer has wires parallel to beam. The two RPC chambers on the outside are also visible.

space resolution of $\sim 100 \mu\text{m}$ and an angular accuracy on a local muon track segment of $\sim 1 \text{ mrad}$ is achieved per station. Meantimer circuits provide a time resolution of a few nanoseconds as needed to identify the bunch crossing with a periodicity of 25 nsec. About 250 such drift chambers of typically $2 \text{ m} \times 3 \text{ m}$ are needed per the barrel; mass production of these chambers is nearing completion in Aachen, Madrid, Padova and Torino. The mounting of barrel muon stations within the barrel yoke wheels has been started in mid-2004 (Fig. 13) and at present the commissioning is proceeding with cosmics.

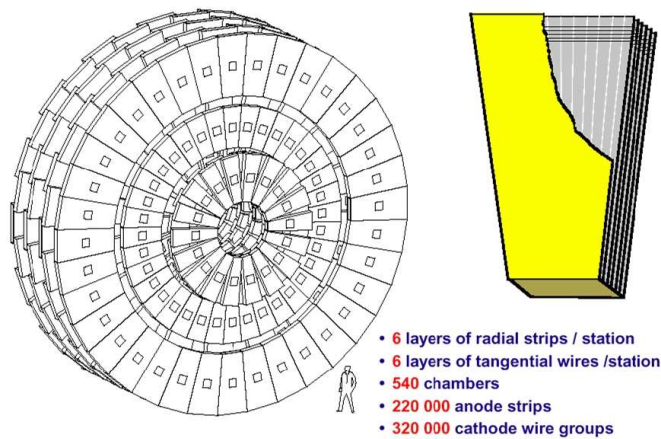


Fig. 13. Arrangement of cathode strip chambers on the endcap yoke and sketch of a CSC.

For the endcaps, Figs. 8 and 14, due to the high magnetic field and high particle rates, cathode strip chambers have been chosen for precise spatial and timing information [10]. The endcap muon system consists of 540 trapezoidal chambers roughly 1 m wide and 2.5 m long (Fig. 14). Each of the modules contains six layers, with strips running radially and wires for timing perpendicular to the strips (Fig. 14). A typical chamber has about 1000 readout channels. The mass production and assembly in the various centres (Fermilab, PNPI-St. Petersburg, IHEP-Peking, Dubna) has been completed, the chambers shipped to CERN and they are now being mounted on the endcap yoke discs and commissioned with cosmics, $\sim 65\%$ by summer 2005 (Fig. 15).

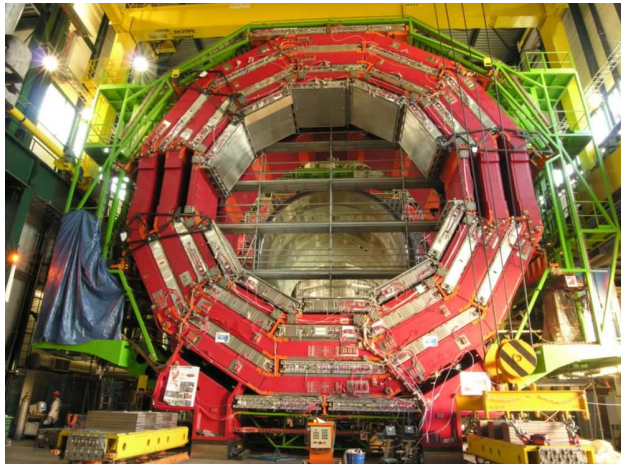


Fig. 14. Mounting of barrel muon stations (DT+RPC) in barrel yoke (YB+2), 34 chambers installed.

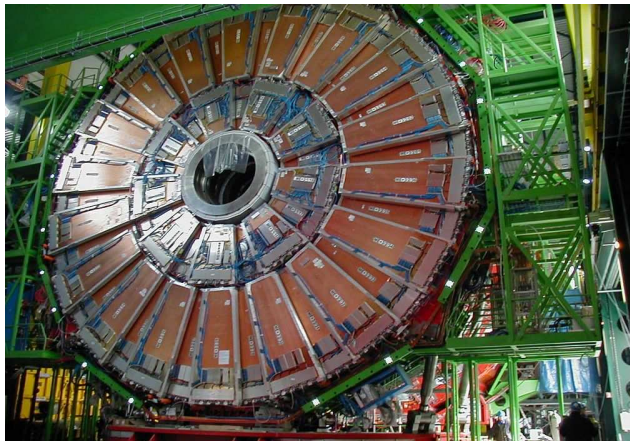


Fig. 15. Mounting of CSC's on end-cap yoke (YE-2) in the CMS surface assembly hall, spring 2005.

The muon trigger is generated in the barrel drift tubes using a meantimer to identify patterns and in the endcaps from cathode strip readout patterns with timing from anode wires. For robustness, in both barrel and endcaps up to rapidity 2.1, the muon stations also include a dedicated muon trigger system based on fast resistive plate chambers (RPC) with a ~ 3 nsec time resolution [10]. The trigger is based on pre-recorded patterns of hits. RPC construction (Italy, China, Korea, Pakistan) is proceeding, by now $\sim 60\%$ have already been manufactured and the installation is going on.

3.3. Tracker

The tracking system of CMS is designed to reconstruct high p_t muons, isolated electrons and hadrons in $|\eta| < 2.4$ with a momentum resolution of $\Delta p_t/p_t \approx 0.15 p_t \oplus 0.5\%$ (p_t in TeV/c). Hadrons must also be reconstructed down to a p_t of ~ 1 GeV/c and also within jets to allow for b-tagging through impact parameter measurements.

Small cell-size silicon pixel and microstrip detectors are used throughout the tracker volume [11]. A sketch of the tracker layout is shown in Fig. 16. Innermost there are three layers of pixel detectors of $100 \mu\text{m} \times 150 \mu\text{m}$ at radii of 4, 7.7 and 11 cm in the barrel, in all 49×10^6 pixels (barrel + endcaps). This pixel detector insures precise impact parameter measurements, with an asymptotic accuracy of $\sigma_{\text{IP}} = 10 - 20 \mu\text{m}$ in the transverse plane.

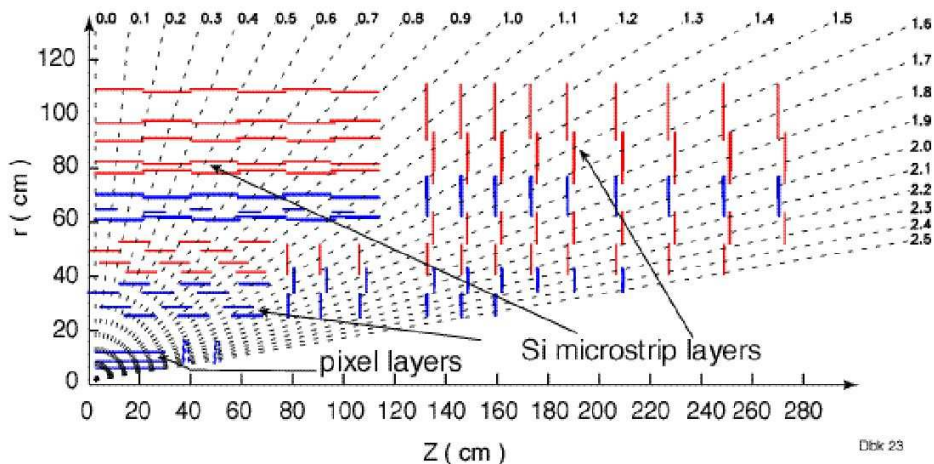


Fig. 16. Layout of one quadrant the all-silicon CMS tracker.

In the barrel region, 10 layers of microstrip Si detectors follow the pixel layers. The pitch varies from 67 to $200 \mu\text{m}$ going outwards; strip lengths vary from 6 to 12 cm. The z coordinate is obtained by a low-angle stereo measurement. Altogether there are $\approx 210 \text{ m}^2$ of silicon sensors with $\approx 9.6 \times 10^6$ microstrip channels. About 17000 modules of 26 different types of $300 \mu\text{m}$ and $500 \mu\text{m}$ thickness have to be

produced in 2 years. The mass production of silicon sensors has been going on at Hamamatsu. With about 9000 sensors of excellent quality produced by now, sensor production should be over by the end of 2005. Some delays are encountered with the manufacture of front-end hybrids. The tracker has to be assembled and installed (except for pixels) by the end of 2006. All carbon-fibre mechanical structure has been delivered and module integration has started. Figure 17 shows part of the tracker inner barrel (TIB) shell being equipped and the assembly of an endcap petals (TEC).

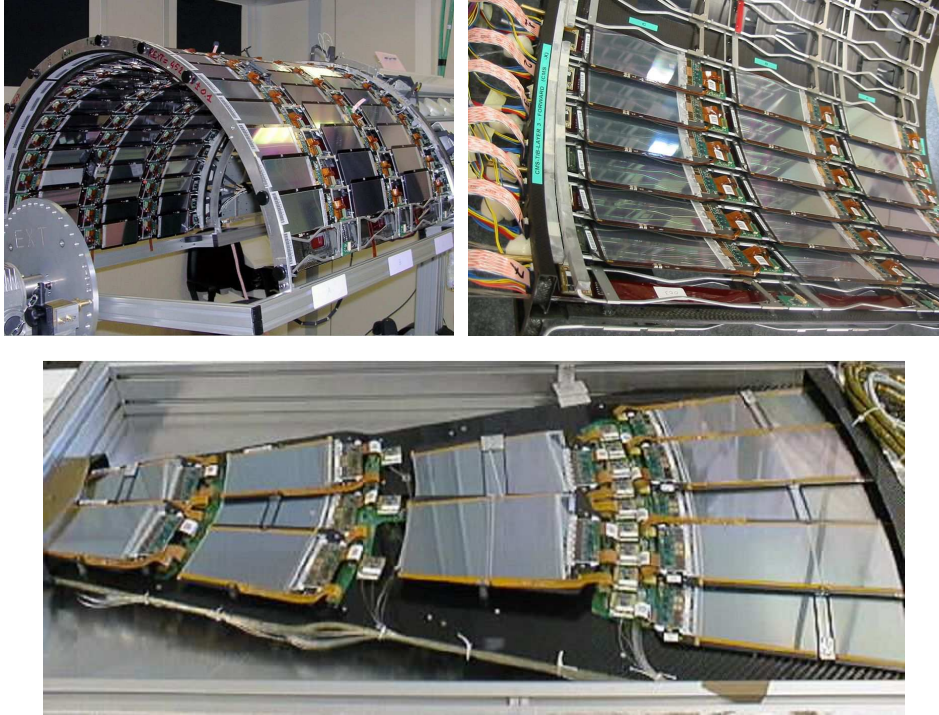


Fig. 17. Tests of assembly of tracker inner barrel modules (TIB) in Pisa (top) and of tracker endcap petals (Lyon) (bottom).

The expected momentum resolution in the tracker alone is $\sim 1-2\%$ for tracks of $10-100 \text{ GeV}/c$ for pseudorapidities < 1.75 . The expected b-tagging efficiency and sample purity has been studied in detail [11]. For b-jets in $t\bar{t}$ events, the efficiency is $\sim 30-50\%$, whilst the expected fake rate probability is $\sim 0.3-1\%$.

3.4. Electromagnetic calorimeter

The main task of the electromagnetic calorimeter (ECAL) is to measure precisely electrons and photons. The goal is to have a $\gamma\gamma$ mass resolution $\sigma_M \sim 1 \text{ GeV}/c^2$. at $10^{34} \text{ cm}^{-2} \text{ s}^{-1}$.

The electromagnetic calorimeter system of CMS is made of high-resolution lead-tungstate (PbWO_4) scintillating crystals extending up to $|\eta| = 3.0$, and a Si preshower in the endcap region $1.5 < |\eta| < 2.5$ [12]. The high density of PbWO_4 crystals (8.3 g/cm^3), with a small Moliere radius of 2.2 cm and a short radiation length of 0.9 cm makes it also possible to have a very compact calorimeter. The arrangement of crystals is shown in Figs. 8 and 18. In the barrel, the crystals are $26 X_0$ deep, the lateral granularity is $\approx 2.2 \text{ cm} \times 2.2 \text{ cm}$, i.e., $\Delta\eta \times \Delta\phi = 0.0175 \times 0.0175$. As the intrinsic light yield of PbWO_4 is low, crystals have to be read-out with photo-detectors with gain. In the barrel, crystals are read out with Si avalanche photodiodes (APD's) [12] and in the endcaps, where the radiation dose is much higher, with vacuum photo-triodes (VPT) [12]. The total number of crystals is $\approx 76 \times 10^3$.

Large-scale production of crystals started in 2000, and by mid-2005 about 38000 crystals have been produced (Bogorodjisk/Russia). At the present rate of ~ 1000 crystals/month, the ECAL endcaps ($\sim 15\text{k}$ crystals) might not be ready for the test run of 2007, but should be there for the physics run in early 2008. To insure timely completion of the ECAL, a fraction ($\sim 10\%$) of crystals are being produced in China (SIC). Avalanche photodiode production at Hamamatsu, has already been completed (130k APD's). Industrial production of VPT's for the endcaps is now under way, about 70% (of the 15 000) have already been delivered and tested. The assembly of ECAL modules and supermodules – each comprising 1700 crystals – is proceeding in the regional centers in Rome and CERN (Fig. 19). Out of the 36 needed, 18 bare supermodules have already been assembled. The front-end chip (FPPA) has been redesigned in $0.25 \mu\text{m}$ technology. The new design (MPGA) reached the target resolution with a noise term of $130 \text{ MeV}/E$ for a 3×3 crystal matrix. The energy resolution obtained in a test beam is $\sigma(E)/E = 3\%/\sqrt{E} \oplus 130 \text{ MeV}/E \oplus 0.4\%$.

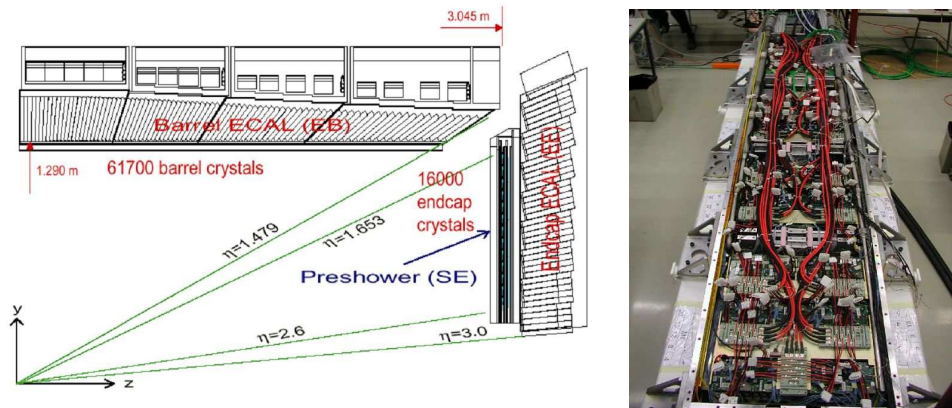


Fig. 18 (left). Longitudinal cut through the electromagnetic calorimeter, with the preshower in front of the endcap crystals. The modular structure of the calorimeter is also clearly visible.

Fig. 19. First ECAL supermodule (SM1) readied for test beam, summer 2004.

3.5. Hadron calorimeters

Hadron calorimetry with large geometrical coverage for measurement of multi-jet final states and missing transverse energy is essential in all sparticle searches, as it is the missing E_t which provides evidence for the escaping LSP-neutralinos.

The hadron calorimeter of CMS in the $|\eta| < 3.0$ region is made of brass absorber plates interleaved with scintillator tiles read-out with embedded wavelength shifting fibers [13]. The readout is done with hybrid photo-detectors (HPD) [13]. In both barrel and endcaps, the tiles are organized in towers (Fig. 8) giving a lateral segmentation of $\Delta\eta \times \Delta\phi \approx 0.09 \times 0.09$. All HCAL wedges have been fabricated (in Felguera, Spain) and delivered to CERN where both half-barrels have been assembled (Fig. 20). The hadron calorimeter endcaps (Fig. 8) have been machined in Minsk, and both have also been delivered at CERN (Fig. 21). The optical elements, manufactured in Fermilab (barrel) and Protvino (endcaps) have been mounted. The mass production of HPD's (DEP, Netherlands) is almost finished. Electronics integration started and source calibration should start very soon. The hadronic resolution obtained in a test beam is $\sigma_E/E \approx 125\% / \sqrt{E} \oplus 5\%$ for the combined ECAL-PbWO₄ and hadronic calorimeter system.



Fig. 20 (left). Half of the barrel hadron calorimeter in its cradle, prepared for test installation.

Fig. 21. Hadron calorimeter endcap mounted on the “nose” of the endcap yoke.

In the forward region, $3.0 < |\eta| < 5.0$, quartz-fiber ‘very forward calorimeters’ (Fig. 8) are used [13]. Their function is to insure detector hermeticity for good

missing transverse energy resolution, and to extend the forward jet detection of CMS. The mass production of forward calorimeter wedges at Tcheljabinsk (Russia) is finished, one HF module is assembled and the second is nearing completion; the photomultipliers for HF readout have been delivered.

3.6. Trigger and data acquisition

At $\sqrt{s} = 14$ TeV and with a luminosity of 10^{34} $\text{cm}^{-2}\text{s}^{-1}$ at the bunch crossing frequency of 40 MHz and with a non-diffractive inelastic pp cross section of 55 mb, we expect on the average about 20 pp collisions per bunch crossing. The trigger/DAQ systems for the LHC experiments thus present an unprecedented challenge, they must look every second at the 40×10^6 crossings, choose the ~ 100 most interesting ones and store them. Thus a selection of trigger thresholds must be made at the various trigger levels to preserve the interesting physics in face of the huge QCD jet background production rates.

CMS has an innovative trigger/DAQ architecture, with basically two selection systems [5]. The main components of the trigger and data acquisition system of CMS are the front-end electronics, the muon and calorimeter first level trigger processors, the readout network and the online event filter system. The 40 MHz collision rate is reduced by the hard-wired first-level trigger system [14] to a level-1 output rate of 30 to 50 kHz by selecting on the simplest detectors and with a coarser granularity on candidate muons, electrons/photons, tau-jets, jets, missing energy or a combination of these basic elements. The front-end electronics and first level trigger processors are pipelined with a pipeline depth of ~ 3 μsec , the time available for this first trigger decision. The higher-level triggers in CMS are all software implemented [15]. The full event is assembled in a memory and selection is made with software algorithms. The event builder, a large (512×512 ports) switching network with a throughput of 500 Gbits/s, feeds the event filter which is made of a large number ($\sim 2 \times 10^3$) of commercially available processors organized into a farm [5,14,15] with a total computing power of 5×10^6 MIPs. A single CPU processes one event. A typical event size is 1 Mbyte. At ‘level-2’, the basic calorimetric and muon triggers are refined, the thresholds are sharpened using full detector granularity, whilst the pixel and microstrip tracker information is used at ‘level-3’. This second – software implemented – event filter stage is capable of accepting data from the first level trigger at an input rate of 75 kHz and reduces the data rate down to about 100 Hz to match the data taking capability of the mass storage devices. The DAQ system is modular, it is subdivided into 8 slices, 4 to 6 of which will be staged for the initial low luminosity ($\sim 10^{32-33}$ $\text{cm}^{-2}\text{s}^{-1}$) running period.

4. Some physics expectations for the LHC

4.1. Higgs boson expectations, SM and MSSM

The main task at the LHC will be to investigate the mechanism responsible for electroweak symmetry breaking. Both ATLAS and CMS have studied in great

detail the observability of the SM Higgs in its various decay modes $H \rightarrow \gamma\gamma$, $b\bar{b}$, $WW (\rightarrow \ell\nu\ell\nu)$, $ZZ^*/ZZ (\rightarrow 4\ell^\pm)$ etc. [5,16,17]. In fact, both detectors CMS and ATLAS have to a large extent been designed and optimized in view of Higgs boson searches.

Figure 22 shows the expected $H \rightarrow \gamma\gamma$ signal in the CMS electromagnetic calorimeter with the expected background level [17]. This mode is the most appropriate one for a Higgs boson search in the ~ 110 to ~ 130 GeV/c^2 mass range, but requires a $\sim 1\%$ $\gamma\gamma$ mass resolution. Another channel allowing exploration of this mass range is $H \rightarrow b\bar{b}$. Figure 23 shows expectations for a 115 GeV/c^2 Higgs produced in $t\bar{t}H$ final states from a fast simulation study [17]. For larger Higgs masses – in fact for the full range $\sim 125 - 700$ GeV/c^2 – the channel $H \rightarrow ZZ^*/ZZ (\rightarrow 4\ell^\pm)$ is the best one (Fig. 24). In CMS the expected 4-lepton mass resolution is ~ 1 GeV/c^2 . Another channel suitable to explore the $\sim 120 - 180$ GeV/c^2 mass range is $H \rightarrow WW \rightarrow \ell\nu\ell\nu$, particularly when produced via the weak boson fusion mechanism $qq \rightarrow qqH$. From the two final-state leptons and the missing transverse energy, it is possible to reconstruct a transverse mass with a Jacobian peak behavior [17].

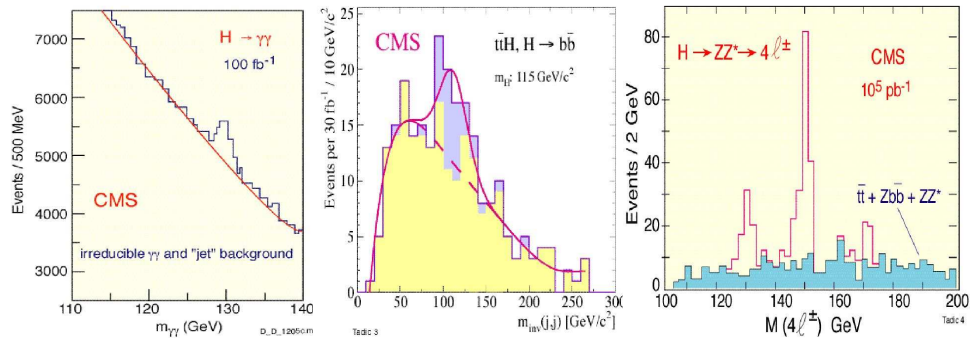


Fig. 22 (left). Reconstructed $H \rightarrow \gamma\gamma$ signal for $m_H = 130$ GeV/c^2 in the CMS crystal calorimeter for an integrated luminosity of 100 fb^{-1} with the expected background level [17].

Fig. 23 (centre). Expected $H \rightarrow b\bar{b}$ signal from $t\bar{t}H$ production ($m_H = 115$ GeV/c^2) for a luminosity of 30 fb^{-1} [17].

Fig. 24 (right). Reconstructed four-lepton invariant mass for the $H \rightarrow ZZ^* \rightarrow 4\ell^\pm$ ($4e^\pm/\mu^\pm$) signal for $m_H = 130, 150$ and 170 GeV/c^2 and the expected background for an integrated luminosity of 100 fb^{-1} [17].

The outcome of the various studies made is summarized in Fig. 25. It gives the expected SM Higgs boson signal significance for 30 fb^{-1} according to CMS expectations. The 5σ signal observation levels for integrated luminosities of 2 and 10 fb^{-1} are also shown. The SM Higgs boson cannot escape detection over the entire expected mass range. The region $200 < m_H < 600$ GeV/c^2 can be explored with less than 10 fb^{-1} . Most demanding is the region $m_H < 125$ GeV/c^2 which relies on the $H \rightarrow \gamma\gamma$ and $H \rightarrow b\bar{b}$ modes, and requires $> 10 - 30$ fb^{-1} , depending on m_H .

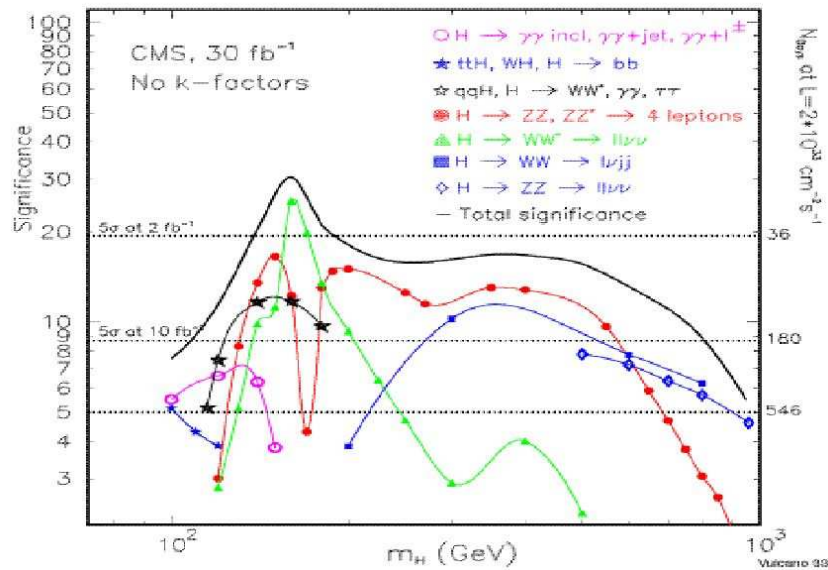


Fig. 25. Expected statistical significance with 30 fb^{-1} for the SM Higgs boson versus m_H according to CMS expectations; the reach for 2 and 10 fb^{-1} is also shown [17].

The observability of the five MSSM Higgs bosons (h, H, A, H^\pm) throughout the parameter space has been studied in great detail [5,16–18]. For MSSM Higgs bosons, some additional decay modes appear, such as $h, H, A \rightarrow \tau\tau$ or $H^\pm \rightarrow \tau\nu$, requiring detection of τ 's in final states, or $h, H, A \rightarrow \mu\mu$ which plays no role in SM Higgs boson searches. The potential importance of τ -final states – in particular with hadronic τ decays – made it necessary to develop specific level-1 and higher-level trigger algorithms to optimize efficiency for hadronic τ 's [14,15]. Another distinctive feature of MSSM Higgs boson production is the importance of $b\bar{b}H_{\text{SUSY}}$ -associated production final states, especially at large $\tan\beta$. The need to detect and identify (b-tag) efficiently, these relatively soft accompanying b-jets have also played a major role in the final optimization of the pixel/microvertexing part of the CMS tracker [11]. An example of the importance of both detecting τ 's and good b-tagging is the search for the charged H^\pm produced in $tH^\pm b$ final states and decaying to $H^\pm \rightarrow \tau\nu$ final states, Fig. 26 [17,18]. The main background is $t\bar{t}$ production. Use of the signal τ polarization, reflecting itself in the π^\pm kinematics in $\tau \rightarrow \pi\nu$ decays, allows to suppress significantly the background. In the tH^\pm final states with a purely hadronic $t \rightarrow bqq$ decay, the main contribution to event E_t^{miss} comes from the parent $H^\pm \rightarrow \tau\nu$ decay, allowing H^\pm transverse mass reconstruction (Fig. 26).

Coverage of parameter space in some of the MSSM Higgs boson searches at luminosities of 30 and 100 fb^{-1} according to CMS expectations is shown in Fig. 28 [17,18]. The entire $\tan\beta - m_A$ MSSM parameter space can be explored with less than 30 fb^{-1} and at least one of the MSSM Higgs bosons can always be found. There are large parts of parameter space where several Higgs bosons can be found, especially at large $\tan\beta$ (> 10) where $A/H/H^\pm$ masses up to $500 - 800 \text{ GeV}/c^2$

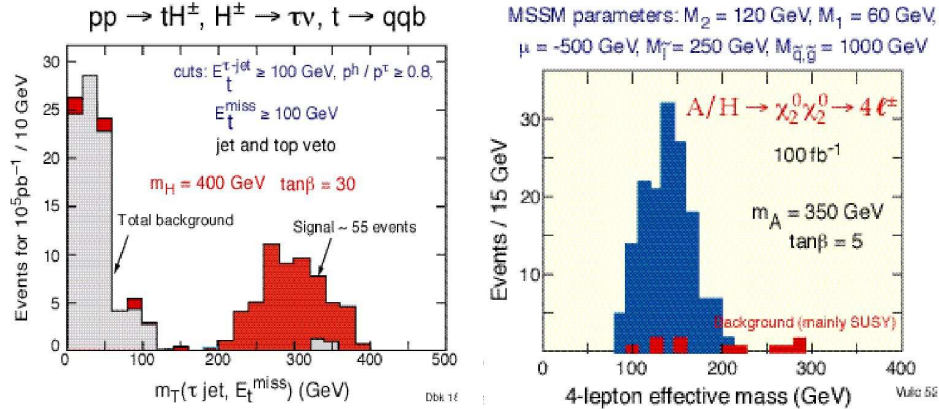


Fig. 26 (left). $H^\pm \rightarrow \tau\nu$ transverse mass reconstruction in tH^\pm final states with hadronic $t \rightarrow bq$ decays.

Fig. 27. Four lepton mass from $H, A \rightarrow \tilde{\chi}_2^0 \tilde{\chi}_2^0 \rightarrow 4\ell^\pm + E_t^{\text{miss}}$ final states.

are within reach with 100 fb^{-1} . The role and importance of τ 's in $h, H, A \rightarrow \tau\tau$ or $H^\pm \rightarrow \tau\nu$ searches is evident, as these are the channels allowing to explore the largest portions of parameter space and giving access to largest $A/H/H^\pm$ masses. Possibilities to observe sparticle decay modes, such as $H, A \rightarrow \tilde{\chi}_2^0 \tilde{\chi}_2^0 \rightarrow 4\ell^\pm + E_t^{\text{miss}}$ or $H^\pm \rightarrow \tilde{\chi}_i^\pm \tilde{\chi}_j^0 \rightarrow 3\ell^\pm + E_t^{\text{miss}}$ are also investigated [17,19]. The channel $H, A \rightarrow \tilde{\chi}_2^0 \tilde{\chi}_2^0$ is particularly interesting. Figure 27 shows the four isolated leptons effective mass at one point in parameter space in the presence of expected (SUSY) backgrounds. This channel would allow – at least in a domain of MSSM mass parameters – to explore a region complementary to $H, A \rightarrow \tau\tau$, as visible comparing Figs. 28a and 28b.

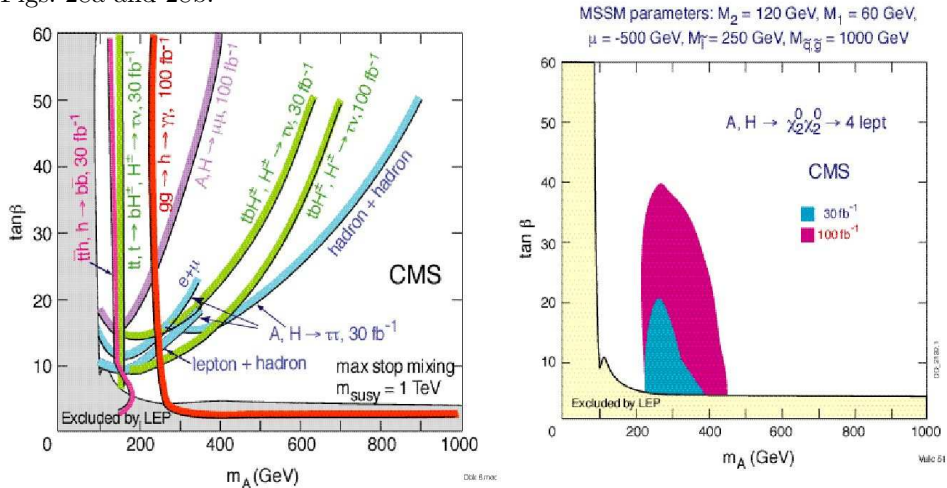


Fig. 28. Coverage of parameter space in various MSSM Higgs boson searches at luminosities of 30 and 100 fb^{-1} : (left) for Higgs boson decays to SM particles, (right) for A/H decays into neutralino pairs at the specified point in parameter space.

4.2. Sparticle studies for LHC

The next most important task at the LHC will be to look for sparticles, i.e. the supersymmetric partners of the SM particles [16,20]. In supersymmetric theories with R-parity conservation, sparticles are pair-produced and there is a stable lightest supersymmetric particle, the LSP. This LSP ($\tilde{\chi}_1^0$), it is an excellent particle physics candidate for cosmological dark matter.

Studies of sparticle observability have been performed most often within the minimal supergravity-constrained MSSM model (mSUGRA) due to its simplicity. The strongly-interacting squarks and gluinos are abundantly produced in pairs $q\bar{q}$, $g\bar{g}$, up to large sparticle masses of the order of 2 TeV. The chargino-neutralino ($\chi_1^\pm \chi_2^0$) direct electroweak (Drell-Yan) pair-production cross sections are also large enough to allow gaugino detection in a significant mass range at the LHC. In all R-parity-conserving sparticle production channels, there is always at the end of the sparticle decay chains production an LSP ($\tilde{\chi}_1^0$). These weakly-interacting massive $\tilde{\chi}_1^0$'s escape direct detection in detectors and their presence is signaled by a missing transverse energy E_t^{miss} . The first experimental evidence for a (R-conserving) SUSY signal will most likely be the observation of an excess of events with significant missing- E_t over expected SM backgrounds.

A systematic study has been done of SUSY signal observability and of the sparticle mass reach in various final states containing leptons, jets and E_t^{miss} and for different integrated luminosities [20]. As an example, Fig. 29 shows the 5σ squark and gluino discovery contours at large $\tan\beta$ for various integrated luminosities

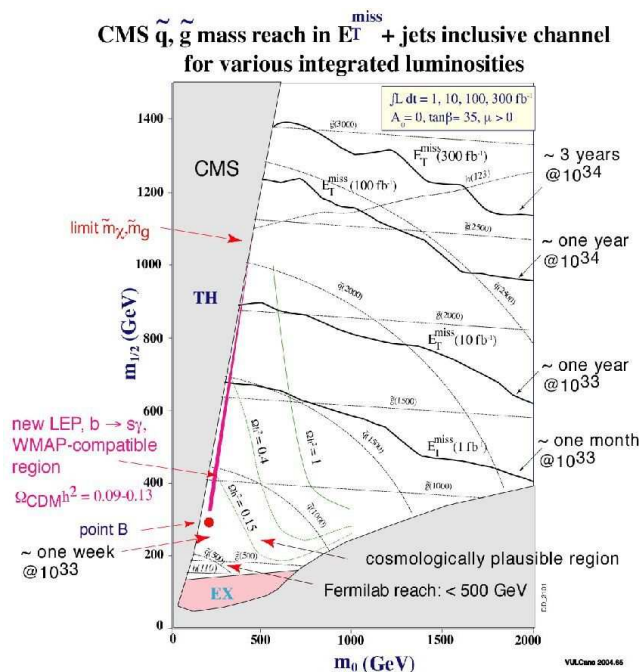


Fig. 29. Example of squark and gluino mass reaches with 1 to 300 fb^{-1} ($\tan\beta = 35$, $\mu > 0$) and LHC running time required; the regions of cosmological interest (WMAP compatible) from the SUSY dark matter point of view are indicated.

ties ranging from 1 to 300 fb^{-1} in final states with at least two central jets and E_t^{miss} of at least 100 GeV. The required LHC running time to achieve a given sensitivity is indicated. Squark and gluino isomass curves are also shown and the mass range which can be explored goes up to $\sim 2.5 \text{ TeV}$. Even a modest LHC running time can greatly extend the Fermilab SUSY mass reach thanks to the almost order of magnitude larger center-of-mass energy.

The WMAP data strongly constrain the dark matter content of the Universe [21] and thereby the supersymmetric scenarios, assuming the $\tilde{\chi}_1^0$ is the cold dark matter particle and thus absolutely stable. Figure 29 shows, taking into account the new WMAP constraints and all the constraints on SUSY from laboratory experiments [22] that only a small band (pink line) of parameter space would still be allowed. The study of Ref. [22] would suggest that SUSY is most likely within the reach of the LHC, except for large values of $\tan\beta$ ($\gtrsim 35$) where some limited regions of parameter space compatible with WMAP cold dark matter results would still extend beyond the LHC kinematical and luminosity reach.

4.3. Dilepton edges and sparticle mass reconstruction

Despite escaping LSP's, sparticle mass reconstruction is possible under some conditions. The method exploiting the sharp edge (endpoint) in the dilepton mass spectrum from the $\tilde{\chi}_2^0 \rightarrow \ell^+ \ell^- \tilde{\chi}_1^0$ decay is well known [23]. The different-flavor dilepton spectra are dominated by uncorrelated sparticle decay dileptons reproducing well the background shape. Figure 30 shows how, at a value of $\tan\beta = 15$ at a specific point in parameter space, in a combination of dilepton spectra, adding

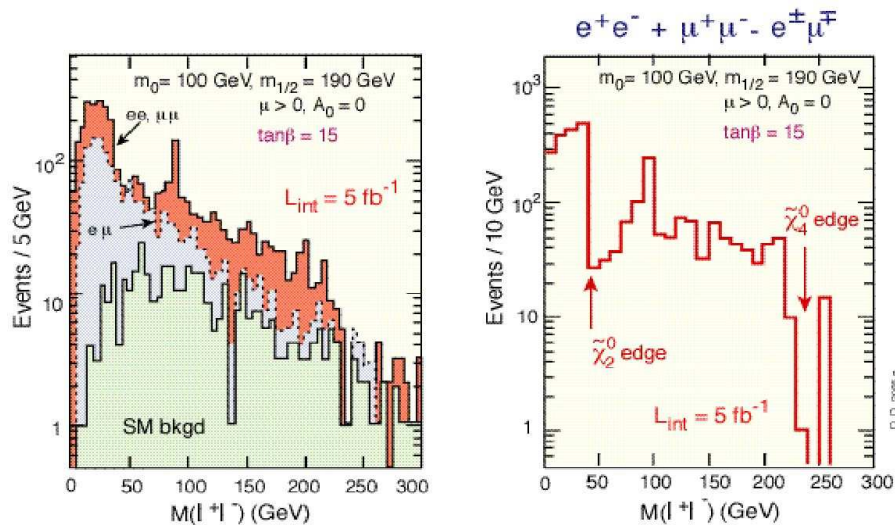


Fig. 30. (left) Opposite-sign dilepton effective mass distributions at $\tan\beta = 15$ for 5 fb^{-1} . Full histogram is for same flavor dileptons, the dashed one for different flavors. (right) Combination of opposite-sign ee , $\mu\mu$ and $e\mu$ spectra, with uncorrelated SUSY and SM backgrounds canceling out displaying two neutralino edges.

e^+e^- and $\mu^+\mu^-$ and subtracting $e^+\mu^-$ and $e^-\mu^+$, the uncorrelated SUSY decays and SM background contributions statistically cancel out, the $\tilde{\chi}_2^0$ -generated edge appears clearly and even a second edge due to $\tilde{\chi}_4^0$ decay appears too.

The domain of parameter space where the dilepton ($ee, \mu\mu$) spectrum is showing, this prominent edge has been mapped for several sets of mSUGRA parameters [20,24]. Figure 31a shows the domains where the dilepton edge is visible with 100 fb^{-1} for $\tan\beta = 2$. The structure in the $\ell^+\ell^-$ spectrum is clearly visible up to $m_{1/2} \approx 900 \text{ GeV}/c^2$ for $m_0 < 400 \text{ GeV}/c^2$. Figure 31b gives the region of observability of the dilepton low-mass enhancement for $\tan\beta = 35$ and 100 fb^{-1} .

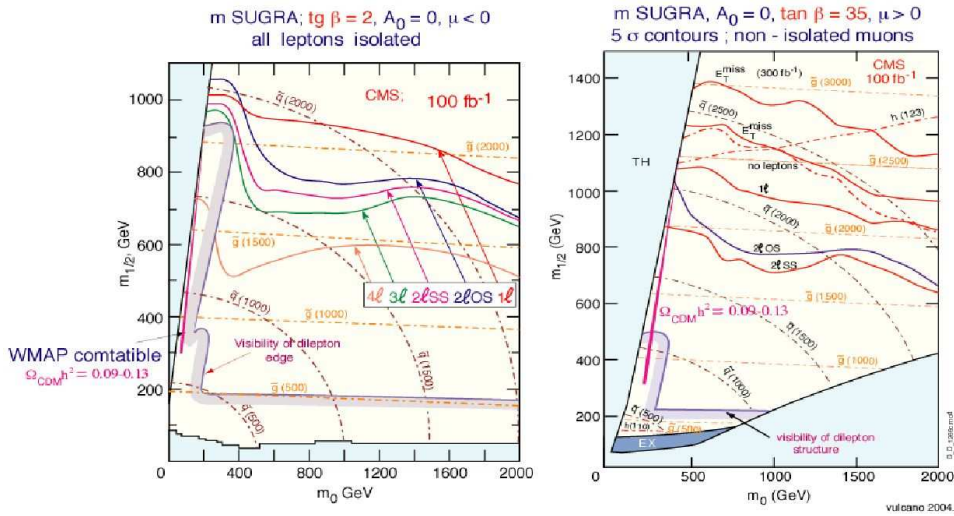


Fig. 31. Two examples of domains (within the shaded boundary) where dilepton structures can be observed in inclusive $\ell^+\ell^- + E_t^{\text{miss}}$ final states, an edge at low $\tan\beta$ or a dilepton low mass enhancement at high $\tan\beta$. The domains of parameter space that can be explored in various topologies depending on the number of leptons are indicated. The regions of compatibility with the WMAP cold dark matter values are also shown.

In favorable cases, the cascade of sparticle decays allows to reconstruct slepton, neutralino, squark, gluino masses with 1% level mass resolutions. In the simplest case, from $\tilde{\chi}_2^0 \rightarrow \ell^+\ell^-\tilde{\chi}_1^0$ decay induced dilepton edges, it is possible, by choosing events at the edge, to reconstruct the parent $\tilde{\chi}_2^0$ momentum [23]. It is then possible to reconstruct the upstream \tilde{q}_L mass from the $\tilde{q}_L \rightarrow q\tilde{\chi}_2^0$ chain by associating the $\tilde{\chi}_2^0$ four-momentum with a nearby q-jet, and finally to reconstruct the $\tilde{g} \rightarrow \tilde{q}q$ decay. A specific example of such reconstructed sparticle masses is shown in Fig. 32 [25] for the SUSY benchmark point B ($m_0 = 100 \text{ GeV}/c^2$, $m_{1/2} = 250 \text{ GeV}/c^2$, $\tan\beta = 10$, $\mu > 0$) and an integrated luminosity of 10 fb^{-1} . If b-jets are selected and associated to the reconstructed $\tilde{\chi}_2^0$, the sbottom is reconstructed ($b\tilde{\chi}_2^0$) and ultimately, requiring another b-jet in the event, the parent gluino decaying to $\tilde{g} \rightarrow \tilde{b}\bar{b} \rightarrow b\bar{b}\tilde{\chi}_2^0$. The mass resolution for both \tilde{b} and \tilde{g} is about 10% for this integrated luminosity.

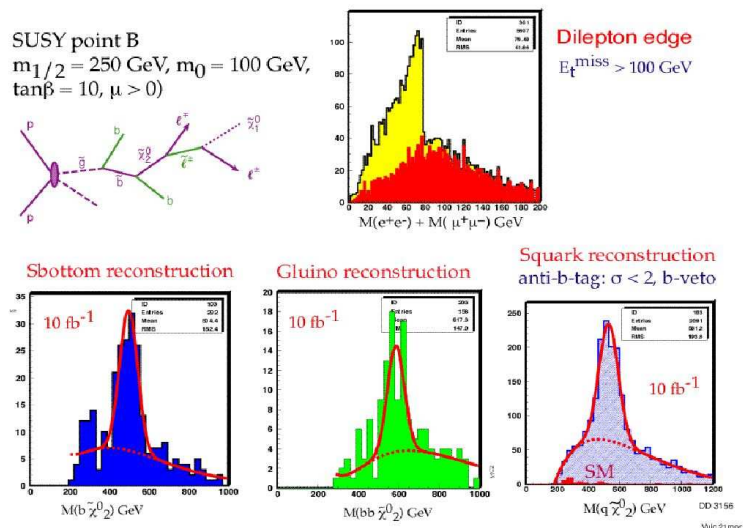


Fig. 32. Example of reconstruction of the \tilde{g} and \tilde{q} masses selecting events in the region of the $\ell^+\ell^-$ edge from $\tilde{\chi}_2^0 \rightarrow \ell^+\ell^-\tilde{\chi}_1^0$ decays, at the SUSY benchmark point B, for 10 fb^{-1} [25]. Hand-drawn backgrounds with fitted signals are shown.

However, more than just the upper dilepton endpoint from $\tilde{\chi}_2^0 \rightarrow \ell^+\ell^-\tilde{\chi}_1^0$ decays can be observed and used in the sparticle reconstruction cascade. A number of particular kinematical configurations generate kinematical lepton and quark-jet end-points and thresholds depending on sparticle mass differences [26]. Provided there is enough statistics and backgrounds are well understood so that these end-points can be clearly measured, including them in a global fit of the full cascade (within a given model, e.g. mSUGRA) provides a more complete information on the model parameters, the sparticle masses and the neutralino mass itself. Such a study has been done in ATLAS at one point in parameter space [27,28]. It shows that with 300 fb^{-1} of integrated luminosity, under favorable model/scenario conditions, the model parameters m_0 , $m_{1/2}$ and $\tan\beta$ could be determined with precisions of $\sim 3\%$, 1% and 0.5% respectively, most of the SUSY spectrum could be reconstructed and the LSP mass could be deduced with a $\sim 10\%$ uncertainty.

5. Conclusions

Civil engineering activities for LHC experiments are finished, all excavations of underground halls are finished and the experimental and service areas delivered for use to experiments. The series production of dipoles from each of the three manufacturers is now proceeding fast, with about 700 of them produced by the summer of 2005.

CMS construction is proceeding at full speed. The CMS magnet yoke is finished, the winding of the coil modules has been completed in 2004 and the cooldown and powering of the magnet and mapping of the field is scheduled for the end of 2005/first months of 2006. The hadron calorimeter and muon systems are on sched-

ule and undergoing commissioning, construction of the electromagnetic calorimeter and tracker is proceeding well, but the schedule is very tight. According to the present expectations, CMS should be closed and ready for data taking (without electromagnetic calorimeter endcaps) for the LHC test runs in the second half of 2007, and the detector should be fully completed for the physics run beginning of 2008.

The main task at the LHC will be to study the mechanism responsible for electroweak symmetry breaking. The ATLAS and CMS detector designs are flexible enough to allow exploring the Higgs mechanism or alternative electroweak symmetry breaking schemes. The LHC is also the most appropriate machine to look for squarks and gluinos, with a mass reach in the $2 - 3 \text{ TeV}/c^2$ range. The LHC allows investigation of a significant fraction of the SUSY sparticle spectrum, and of SUSY Higgs bosons over most of parameter space. Depending on the SUSY scenario possibly realized in Nature, the reconstruction of the sparticle mass spectrum could, however, be a long and tedious task. Clearly a lot of work and checking within the various SUSY LHC measurements will be required to understand consistency of LHC data with a given SUSY scheme or model.

References

- [1] P. W. Higgs, Phys. Rev. Lett. **12** (1964) 132; Phys. Rev. Lett. **13** (1964) 508; F. Englert and R. Brout, Phys. Rev. Lett. **13** (1964) 321; G. Altarelli, *Proc. LHC Workshop*, Aachen, CERN 90-10, 1990 and refs. therein; J. F. Gunion, H. E. Haber, G. L. Kane and S. Dawson, *The Higgs Hunter's Guide*, Addison-Wesley, Redwood City (1990).
- [2] Z. Kunszt and F. Zwirner, Nucl. Phys. B **385** (1992) 3, and references therein; H. P. Nilles, Phys. Rep. **110** (1984) 1; M. Carena et al., CERN-TH/95-45.
- [3] N. Arkani-Hamed, S. Dimopoulos and G. Dvali, Phys. Lett. B **429** (1998) 263, hep-ph/9803315; Phys. Rev. D **59** (1999) 86004; I. Antoniadis et al., Phys. Lett. B **436** (1998) 257; G. Giudice, R. Rattazzi and J. D. Wells, *Quantum Gravity and Extra Dimensions at High-Energy Colliders*, Nucl. Phys. B **544** (1999); L. Randall and R. Sundrum, Phys. Rev. Lett. **83** (1999) 3370, hep-ph/9905221.
- [4] Technical Proposal, ATLAS Collaboration, CERN/LHCC/94-43, LHCC/P2, Dec. 1994.
- [5] Technical Proposal, CMS Collaboration, CERN/LHCC 94-38, LHCC/P1, Dec. 1994.
- [6] Technical Proposal, ALICE experiment, CERN/LHCC 95-71, LHCC/P3, Dec. 1995 and CERN/LHCC96-32, LHCC/P3-Addendum 1, Oct. 96.
- [7] LHCb, Technical Proposal CERN/LHCC 98 LHCC/P4, 20 Feb. 1999; Status of the LHCb Detector Reoptimisation, CERN/LHCC 2003-003; LHCb 2003-006 LHCC.
- [8] G. Baur et al., CMS Collaboration, *Heavy Ion Physics Programme in CMS*, CMS NOTE 2000/060.
- [9] CMS Collaboration, *The Magnet Project, Technical Design Report*, CERN/LHCC 97-10, CMS TDR1, 1997.
- [10] CMS Collaboration, *The Muon Project, Technical Design Report*, CERN/LHCC 97-32, CMS TDR3, 1997.
- [11] CMS Collaboration, *The Tracker Project, Technical Design Report*, CERN/LHCC 98-6, CMS TDR5, 1998; *CMS Addendum to CMS Tracker TDR*, CERN/LHCC 2000-016.
- [12] CMS Collaboration, *The Electromagnetic Calorimeter Project, Technical Design Report*, CERN/LHCC 97-33, CMS TDR4, Dec. 97.

- [13] CMS Collaboration, *The Hadron Calorimeter Project, Technical Design Report*, CERN/LHCC 97-31, CMS TDR2, June 97.
- [14] CMS Collaboration, *The Level-1 Trigger, Technical Design Report*, CERN/LHCC 2000-38, CMS TDR 6.1, Dec. 2000.
- [15] CMS Collaboration, *Data Acquisition and High Level Trigger, Technical Design Report*, CERN/LHCC 2002-26, CMS TDR 6.2, Dec. 2002.
- [16] ATLAS Collaboration, *Detector and Physics performance, Technical Design Report*, CERN/LHCC/99-14 and CERN/LHCC/99-15, May 1999; J.G. Branson et al., *High Transverse Momentum Physics at the Large Hadron Collider*, ATLAS and CMS collaborations, hep-ph/0110021, Oct. 2001.
- [17] S. Abdoullin et al., Eur. Phys. J C **39** (2005) s2, s41s61; *Summary of the CMS Potential for the Higgs Boson Discovery*, CMS NOTE 2003/033, Dec. 2003 and references therein.
- [18] R. Kinnunen, *Higgs Physics at LHC*, CMS CR 2002-020, presented at *SUSY02 10th Int. Conf. on Supersymmetry and Unification of Fundamental Interactions*, DESY, Hamburg, June 2002; D. Denegri et al, *Summary of the CMS Discovery Potential for the MSSM SUSY Higgs*, CMS Note 2001/032; hep-ph/0112045, Dec. 2001.
- [19] F. Moortgat, S. Abdullin and D. Denegri, *Observability of MSSM Higgs bosons via sparticle decay modes in CMS*, CMS Note 2001/042; hep-ph/0112046, Dec. 2001, and references therein; M. Bisset, F. Moortgat and S. Moretti, *Trilepton + top Signal from Chargino-Neutralino Decays of MSSM Charged Higgs Bosons at LHC*, CERN-TH/2002-173, TUHEP-TH-02138.
- [20] S. Abdullin et al., CMS Collaboration, *Discovery Potential for Supersymmetry in CMS*, J. Phys. G: Nucl. Part. Phys. **28** (2002) 469; hep-ph/9806366, and references therein.
- [21] C. L. Bennett et al., *Astrophys. J. Suppl.* **148** (2003) 1 (astro-ph/0302207); D. N. Spergel et al., *Astrophys. J. Suppl.* **148** (2003) 175 (astro-ph/0302209); H. V. Peiris et al., *Astrophys. J. Suppl.* **148** (2003) 213 (astro-ph/0302225).
- [22] J. Ellis, K. A. Olive, Y. Santoso and V. C. Spanos, hep-ph/0303043.
- [23] F. Paige, *Determining SUSY Particle Masses at LHC*, hep-ph/9609373; *SUSY Studies in CMS*, in LHCC SUSY Workshop, CMS Document 1996-149, CERN, Oct. 29-30, 1996; I. Hinchliffe et al., *Phys. Rev. D* **55** (1997) 5520, and references therein.
- [24] D. Denegri, W. Majerotto and L. Rurua, *Phys. Rev. D* **58** (1998) 095010; *Phys. Rev. D* **60** (1999) 035008.
- [25] M. Chiorboli, Ph.D. Thesis, *Supersymmetric Particle Reconstructions with the CMS Detector at LHC*, University of Catania, Italy, 2002; A. Tricomi, *Sparticle Searches with CMS at LHC*, CMS CR 2002/022, presented at *SUSY02, 10th Int. Conf. on Supersymmetry and Unification of Fundamental Interactions*, DESY, Hamburg, June 2002.
- [26] B. C. Allanach et al., *Eur. Phys. J. C* **25** (2002) 113.
- [27] B. C. Allanach, C. Lester, M. A. Parker and B. R. Webber, *JHEP* 0009(2000) 4, hep-ph/0007009; B. K. Gjelste et al., *A Detailed Analysis of the Measurements of SUSY Masses with the ATLAS Detector at LHC*, ATLAS internal note ATL-PHYS-2004-007 (2004), to appear in *LHC/LC Study group document*, ed. G. Weiglein, and ref. therein.
- [28] G. Polesello and D.R. Tovey, *Constraining SUSY Dark Matter with the ATLAS Detector at the LHC*, SHEP-HEP/03-6, Feb. 2004.

EKSPERIMENT CMS NA LHC-u

Opisujemo sadašnje stanje gradnje ubrzivača LHC, napredak u gradnji detektora CMS i neka očekivanja fizičkih istraživanja i traganja na LHC-u.